

Viewpoints

From the Neuroscience of Individual Variability to Climate Change

 Eve Marder and Mara C.P. Rue

Volen Center and Biology Department, Brandeis University, Waltham, Massachusetts 02454

Years of basic neuroscience on the modulation of the small circuits found in the crustacean stomatogastric ganglion have led us to study the effects of temperature on the motor patterns produced by the stomatogastric ganglion. While the impetus for this work was the study of individual variability in the parameters determining intrinsic and synaptic conductances, we are confronting substantial fluctuations in the stability of the networks to extreme temperature; these may correlate with changes in ocean temperature. Interestingly, when studied under control conditions, these wild-caught animals appear to be unchanged, but it is only when challenged by extreme temperatures that we reveal the consequences of warming oceans.

Introduction

Small children learn at an early age to recognize individuals. Consequently, we all grow up with a knowledge of the world that somehow combines our understanding of individual differences in behavior with the implicit assumption that each dog, or each human, will show predictable and consistent responses to their environments in most circumstances. Much of the early data collected in neuroscience came from wild-caught animals; therefore, the diversity in the natural population was reflected in the data obtained. Nonetheless, because of numerous technical advantages, most animal studies in neuroscience today are conducted with genetically inbred strains of mice, flies, and worms. This has led to the implicit expectation, justified or not, that all individuals of the same genotype will be well represented by their means, although this is itself a flawed assumption (Golowasch et al., 2002). Instead, those who study behavior know that genetically identical animals also display animal-to-animal variability in behavior.

We now describe the 20 or so year path that the E.M. laboratory has taken that started with studies of animal-to-animal variability and has brought us to the hidden effects of climate change on the nervous system of the crabs and lobsters, which we have studied for almost 50 years. We started measuring variability in circuit parameters and function in the stomatogastric nervous system (STNS) of crabs and lobsters and their consequences for robust and reliable circuit function. Because we work with wild-caught crabs that live in the varying temperatures of the North

Atlantic Ocean, we have found ourselves inadvertently studying the sequelae of climate change on the nervous systems of the local crab populations. Indeed, the performance of the stomatogastric ganglion (STG) of the crab, *C. borealis*, has become a window onto the long-term effects of the ocean's temperature changes. Here, we trace the intellectual pathway that has led from the most basic of basic neuroscience to climate change.

Degenerate, or multiple solutions, in conductance-based models of neurons and small networks

Neurons typically have many different classes of ion channels that give them their characteristic intrinsic firing patterns. Before the advent of molecular techniques to characterize ion channel genes in single neurons, the identification of the channel complement present in neurons came from biophysical and pharmacological analyses of membrane currents. Studies such as these provided evidence that neurons of the crustacean STG, like many others, have inward Na^+ and Ca^{2+} currents, a hyperpolarization-activated inward current, (I_H) and multiple K^+ currents (Golowasch and Marder, 1992; Turrigiano et al., 1995). Voltage-clamp measurements of these currents were fit with differential equations and then used to construct conductance-based models of STG neurons that typically have 5–7 voltage and time-dependent currents (Epstein and Marder, 1990; Buchholtz et al., 1992; Golowasch and Marder, 1992; Golowasch et al., 1992; Guckenheimer et al., 1993, 1997; Turrigiano et al., 1995; Goldman et al., 2001; Prinz et al., 2003).

While early work on developing conductance-based models focused on fitting the model's performance to a specific target activity pattern, and used tedious hand-tuning of the model's parameters (Buchholtz et al., 1992; Golowasch et al., 1992), it quickly became clear that many different sets of model parameters can produce similar outputs (Liu et al., 1998; Goldman et al., 2001; Golowasch et al., 2002; Alonso and Marder, 2019). Consequently, >20 years ago, we and others began creating families of models that capture the variability and range of the biological data (Goldman et al., 2001; Prinz et al., 2003; Taylor et al., 2006, 2009; Marder and Taylor, 2011).

Received June 18, 2021; revised Oct. 28, 2021; accepted Nov. 1, 2021.

This work was supported by HHS | NIH | National Institute of Neurological Disorders and Stroke (NINDS) NS 097343 to E.M., HHS | NIH | National Institute of Mental Health (NIMH) MH46742 to E.M., and National Institute of Neurological Disorders and Stroke (NINDS) F31 NS 113383 to M.C.P.R.; and the Steven J. Clooback Foundation. We thank all members of the E.M. laboratory, present and past, for all contributions to the laboratory.

The authors declare no competing financial interests.

Correspondence should be addressed to Eve Marder at marder@brandeis.edu or Mara C.P. Rue at mcprue@brandeis.edu.

<https://doi.org/10.1523/JNEUROSCI.1261-21.2021>

Copyright © 2021 the authors

In keeping with the definitions of Edelman and Gally (2001), we call these multiple solutions “degenerate,” as their functional outputs are similar, but the parameters that give rise to these can be quite variable. Perhaps one of the most well-known examples of degenerate solutions to circuit performance was shown in Astrid Prinz’s models of the pyloric rhythm of the STG (Prinz et al., 2004). The core features of the pyloric rhythm of the STG are shown in Figure 1. Figure 1A shows a schematic of how recordings from the dissected STNS are obtained. Intracellular recordings from STG somata are made with glass microelectrodes. The neurons are identified based on their firing patterns and their projections in the motor nerves that exit the STG to innervate specific stomach muscles (Marder and Bucher, 2007). The triphasic pyloric rhythm generates movements that filter food in the animal’s foregut, and consists of alternating activity in the pyloric dilator (PD), lateral pyloric (LP), and pyloric (PY) neurons (Fig. 1B). The PD neurons are motor neurons that dilate the pylorus, while the LP and PY neurons are motor neurons that constrict the pylorus. Figure 1C shows a connectivity diagram for the pyloric rhythm. In this diagram, the filled circles represent chemical inhibitory synapses, and the resistor symbols denote electrical coupling. In the presence of descending modulatory input, the anterior burster (AB) is an intrinsically bursting neuron, and strong electrical coupling to the PD neurons causes them to fire with the AB neuron (Marder and Bucher, 2007). Together, the AB and PD neurons rhythmically inhibit the LP and PY neurons, which fire on rebound from inhibition, accounting for their alternation with the PD neurons.

Prinz et al. (2004) created and simulated >20 million versions of a three cell model of the pyloric rhythm, using a database of 1.7 million neurons whose excitability had been previously characterized (Prinz et al., 2003). Of these, ~400,000 were reasonable models of the pyloric rhythm, in that they captured the range of behaviors of the pyloric rhythms measured from 99 animals (Prinz et al., 2004). Figure 2 shows two of these representative models with pyloric activity and demonstrates that similar circuit performance can result from very different sets of parameters. The top of the figure shows two model circuits with similar outputs. Below are some of the synaptic and intrinsic conductances in these circuits, which are quite different. Taken at face value, this is a demonstration that similar outputs can result from significantly disparate sets of parameters.

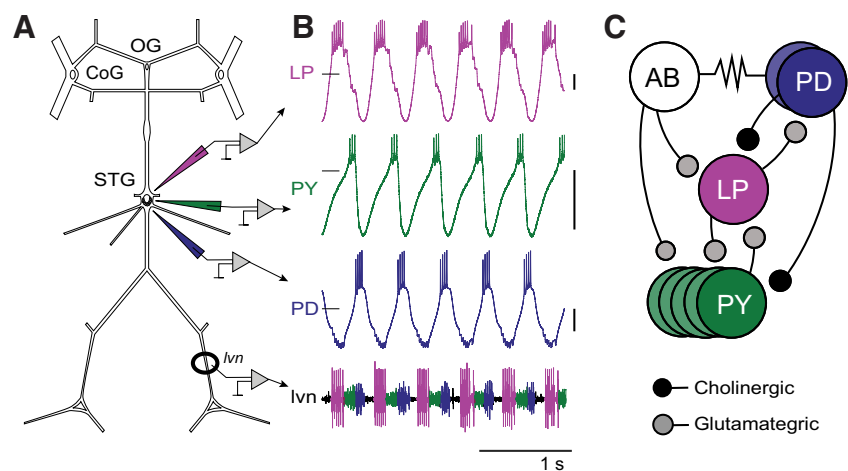


Figure 1. Simplified overview of the STNS and pyloric rhythm in *C. borealis*. **A**, Schematic of the preparation showing the pinned-out STNS. **B**, The triphasic pyloric rhythm with simultaneous recordings from the LP, PY, and PD neurons and extracellular lateral ventricular nerve (lvn), which contains axons from all three neuron types. Recordings made by Sonal Kedia. Horizontal lines indicate -40 mV. Calibration, vertical: 10 mV. **C**, Pyloric circuit connectivity diagram. Filled circles represent chemical inhibitory synapses. Resistor symbol illustrates electrical coupling.

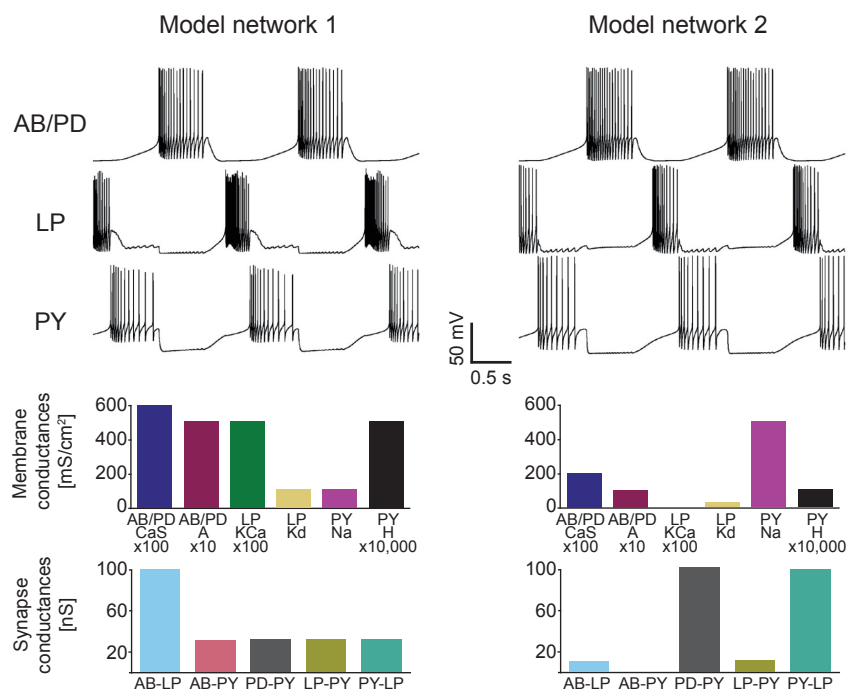


Figure 2. Two model pyloric networks generate very similar activity despite widely differing cell-intrinsic and synaptic properties. Top, Voltage traces from the AB/PD, LP, and PY neurons in two model pyloric networks. Middle, Selected membrane conductances for the above model networks. Bottom, Selected synaptic conductances from the above model networks. Data from Prinz et al. (2004).

This raises a number of important questions, and much of the work we have done since this paper was published has been to answer these questions:

- How variable are the parameters in real biological networks?
- How reliably can animals with intrinsic variability respond to perturbations?
- Do perturbations reveal cryptic animal–animal differences?

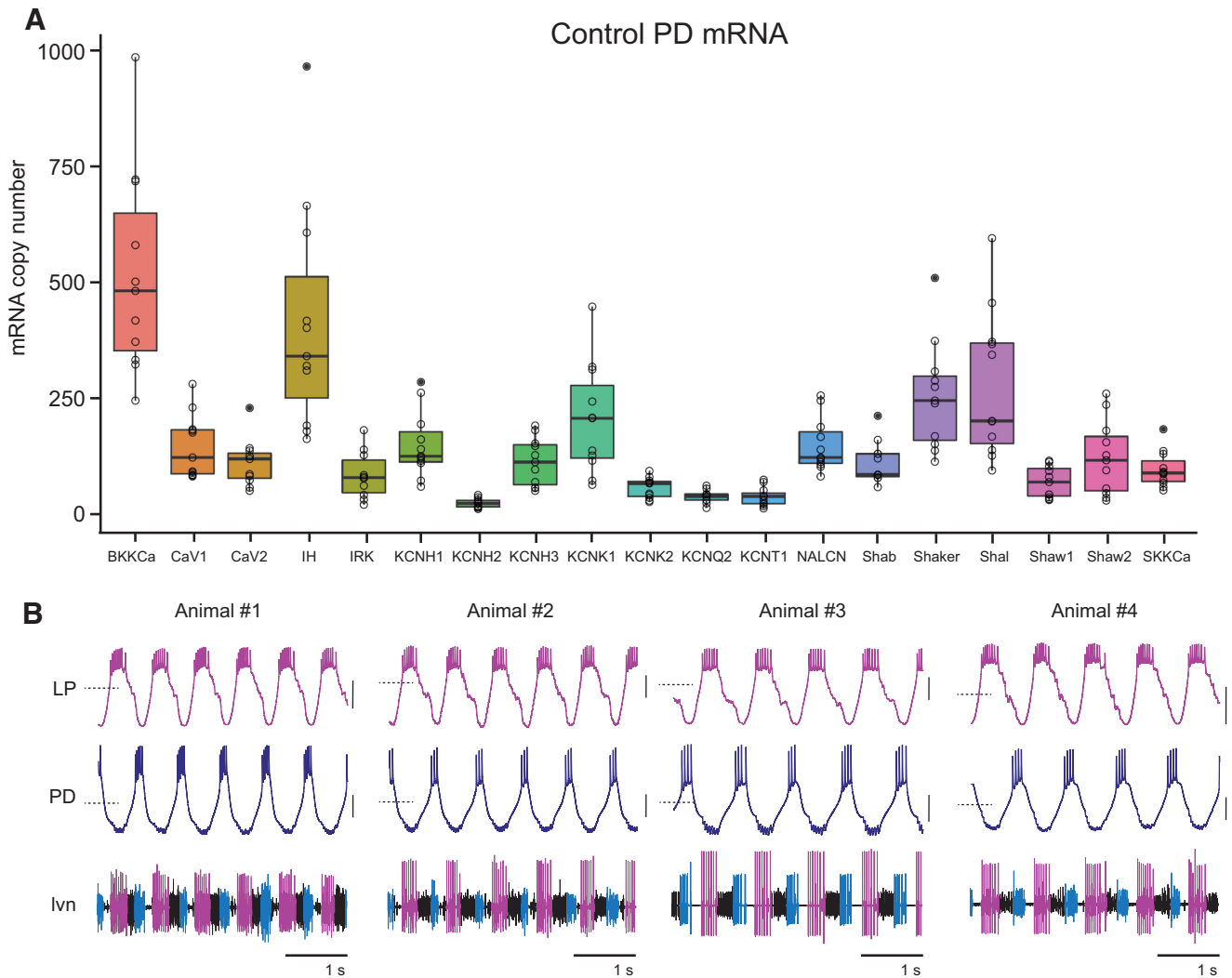


Figure 3. Identified neurons in the STNS display similar baseline activity despite underlying individual variability in ion channel expression. **A**, mRNA copy number for ion channels in single, hand-dissected PD neurons from the crab, *C. borealis*. Data were replotted from a dataset published by Northcutt et al. (2019). **B**, Individual pyloric rhythms are nearly identical across animals. Simultaneous intracellular voltage traces from the LP and PD neurons, and extracellular voltage trace from the lvn nerve are shown for 4 individual animals (#1–4). Calibration, intracellular voltage traces: -40 mV (dashed horizontal), 10 mV scale (vertical). Recordings from M.R.

- Are some sets of parameters associated with higher resilience?

How variable are the parameters in biological networks?

Experimentalists have always dealt with variance in their measurements. The challenge is to distinguish between the intrinsic variability in the measured population, whether they be humans, or synapses, and the variability that is an unwanted consequence of measurement noise. In most, if not all, experimental measurements, the two components are there. A number of lines of reasoning suggest that much of the variability we see is a biological feature.

Theory studies, such as shown in Figure 2 (Goldman et al., 2001; Golowasch et al., 2002; Prinz et al., 2004; Alonso and Marder, 2019, 2020), make it clear that degenerate solutions do exist. Therefore, biological cell-to-cell or animal-to-animal variability is consistent with robust performance in the animal or population. Historically, the theory studies gave us confidence that the kind of variability we routinely saw in the laboratory could be dominated by biological variance.

Figure 3A illustrates the variability in mRNA expression of a number of ion channels in hand-dissected single PD neurons from the STG (Northcutt et al., 2019). In these recent measurements, as in earlier ones (Schulz et al., 2006, 2007), there is a 2- to 6-fold variability in the expression of the channel genes in each cell type. Additionally, but not shown here, there are also cell type-specific sets of correlations in their expression. The 2- to 6-fold variance is similar to what is reported in data from other systems (Amendola et al., 2012; Roffman et al., 2012; Golowasch, 2014; Goaillard and Marder, 2021). Other studies show correlations in ion channel expression and physiological measures (Goaillard et al., 2009; Temporal et al., 2012; Golowasch, 2014; Tapia et al., 2018; Moubarak et al., 2019; Goaillard and Marder, 2021). On balance, only a modest amount of the variance in the data we measure can be attributed to true measurement “noise,” as measurement error would wash out the correlation structures seen in these data.

Despite the considerable amount of variance in all measures of individual conductances, synaptic strengths, or anatomical form (Goaillard et al., 2009; Otopalik et al., 2017a, b, 2019), the control pyloric rhythms across animals are nonetheless quite

similar and reliable (Fig. 3B) (Gorur-Shandilya et al., 2021). This suggests that recordings from healthy animals that generate stereotyped and reliable motor patterns, such as those seen in Figure 3B, are hiding “cryptic” animal-to-animal variability that is invisible until the networks are perturbed (below) or unless revealed when individual circuit parameters are specifically measured.

Some homeostatic models that allow neurons to self-assemble to a target intrinsic activity pattern also result in variable final parameters (Liu et al., 1998; O’Leary et al., 2013, 2014; O’Leary and Marder, 2016). We speculate that the measured 2- to 6-fold variation in parameters across animals, or neurons, or over chronological time represents a trade-off between the size of the manifolds that allow similar outputs and the constraints of biological regulatory processes. It is difficult to imagine that all biological processes can be perfectly tuned to within a few percent at all times in long-lived animals, as membrane proteins are constantly replaced. Likewise, it is clear that systems are not infinitely robust to changes in parameters. Thus, this 2- to 6-fold range in cell and circuit parameters may be the approximate size of the degenerate set of solutions available to a neuron or circuit. It must be remembered that most random sets of parameters are not “good solutions” (Caplan et al., 2014); therefore, biological systems must have mechanisms, such as homeostatic regulation that allow them to find successful solutions (LeMasson et al., 1993; Liu et al., 1998; O’Leary et al., 2013, 2014).

How reliably can animals with intrinsic variability respond to perturbations?

Circuits with similar outputs but different sets of underlying parameters should be differentially sensitive to perturbations, precisely because the mechanisms that give rise to the measured outputs rely more or less heavily on different membrane or synaptic currents. Consequently, we expect that animals or models with different underlying sets of parameters will not be equally able to maintain robust behavior to all possible perturbations. At the same time, we know that genetic deletions of some ion channel genes show little or no phenotype. Presumably this means, at least under control conditions, that there are other genes with sufficiently overlapping functions to allow the output to be maintained over some ranges (Alonso and Marder, 2020).

There are three major classes of perturbations that we and others study to understand circuit dynamics: (1) global perturbations, such as changes in temperature, pH, oxygen levels, and ionic composition of the saline, that will influence all neurons in a circuit, and for some, every protein involved in cellular signaling; (2) changes in one or more parameter, as is often done in sensitivity analyses in models, or occurs as a consequence of some pharmacological agents or neuromodulation; and (3) targeted neuronal deletions, in which individual neurons or groups of neurons are removed from functional circuits. Each of these manipulations is a “perturbation,” but each of these is likely to be informative in different ways. Most importantly, each is likely to reveal different aspects of how degeneracy in the population is related to the individual and the population’s resilience.

To what extent can wild-caught animals, with variable sets of properties, respond reliably and predictably to the perturbations that they encounter in their natural environments? And can that population adapt or acclimate to the environmental changes introduced by climate change or other challenges? In the past 15 years, we have focused our studies on three global perturbations: temperature (Tang et al., 2010, 2012; Rinberg et al., 2013; Soofi et al., 2014; Haddad and Marder, 2018), altered pH (Haley et al., 2018; Ratliff et al., 2021), and high potassium (He et al.,

2020) to study the resilience of STG networks. In each case, we have characterized the effects of the perturbation until it produces disruptions, or crashes, in the normal pyloric rhythm. Changes in temperature and pH are perturbations that crabs routinely experience in their natural environment, and changes in extracellular K^+ concentration occur in human physiology and disease. In the first instance, we studied these singly, but we have also looked at interactions among them (Ratliff et al., 2021).

Temperature compensation is a challenge to the nervous system, and it continues to surprise and awe us that biological systems can deal with large ranges in temperature as well as they do because all ion channels and signaling proteins are temperature-sensitive, albeit to a different degree (Tang et al., 2010; Robertson and Money, 2012). Because neuronal circuit dynamics depend on the timing of activation and inactivation of many ion channels, it is easy to understand that, if the temperature dependencies of the activation and inactivation rates of ion channels are not appropriately matched, neurons and the circuits in which they are found, will “crash” or become dysfunctional in response to alterations in temperature (Tang et al., 2010; O’Leary and Marder, 2016). Indeed, it is nontrivial to find computational models that are robust to temperature (Caplan et al., 2014). Two studies have successfully found temperature-robust models, either using the correlations that result from a homeostatic model (O’Leary and Marder, 2016) or by using genetic algorithms to specifically find temperature-robust solutions (Alonso and Marder, 2020).

In our first experimental studies on the effects of temperature, we found normal pyloric rhythms for temperatures between 7°C and 24°C (Tang et al., 2010, 2012), but disrupted rhythms at higher temperatures (Fig. 4). Although all animals produce very similar rhythms under control conditions (Fig. 3B), they crash with quite different dynamics, and generate noticeably different patterns as they crash. Figure 5A shows this for four biological preparations that crashed at temperatures warmer than 23°C. Although all preparations crashed, each of them crashed at a different temperature. Similar results are seen in four model networks in which each model has a different set of parameters (Fig. 5B, Alonso and Marder, 2020). Thus, we assume that the diversity of crash dynamics and temperatures shown by the biological preparations is attributable to their underlying synaptic and intrinsic conductances, as is also the case for the models. Importantly, all animals respond reliably and robustly to the range of temperatures that they typically encounter in the wild.

Thus far, we have focused on the rapid pyloric rhythm of the STG. The STG also generates a slower, gastric mill rhythm. While the pyloric rhythm is generated by the activity of a set of bursting pacemaker neurons, the gastric mill rhythm depends on the activity of a set of descending modulatory neurons that are themselves activated by sensory inputs (Beenhakker et al., 2004, 2007; Blitz and Nusbaum, 2012), and reciprocal inhibition is at the core of this rhythm. Figure 6 shows extracellular recordings from motor nerves containing elements of the gastric rhythm (the lgn shows activity of the lateral gastric [LG] neuron, and the dgn shows activity of the dorsal gastric neuron). The pdn shows activity of the PD neurons, so comparing the frequency of the LG activity to the PD activity illustrates the difference in periods of the two rhythms. Figure 6 uses color to illustrate the effects of temperature on both rhythms, and demonstrates that the gastric mill rhythm can also operate over a relatively wide range of temperatures (Powell et al., 2021). Indeed, although the pyloric and gastric mill rhythms differ in period by about a factor of 10, their dependence on temperature is similar (Powell et al., 2021).

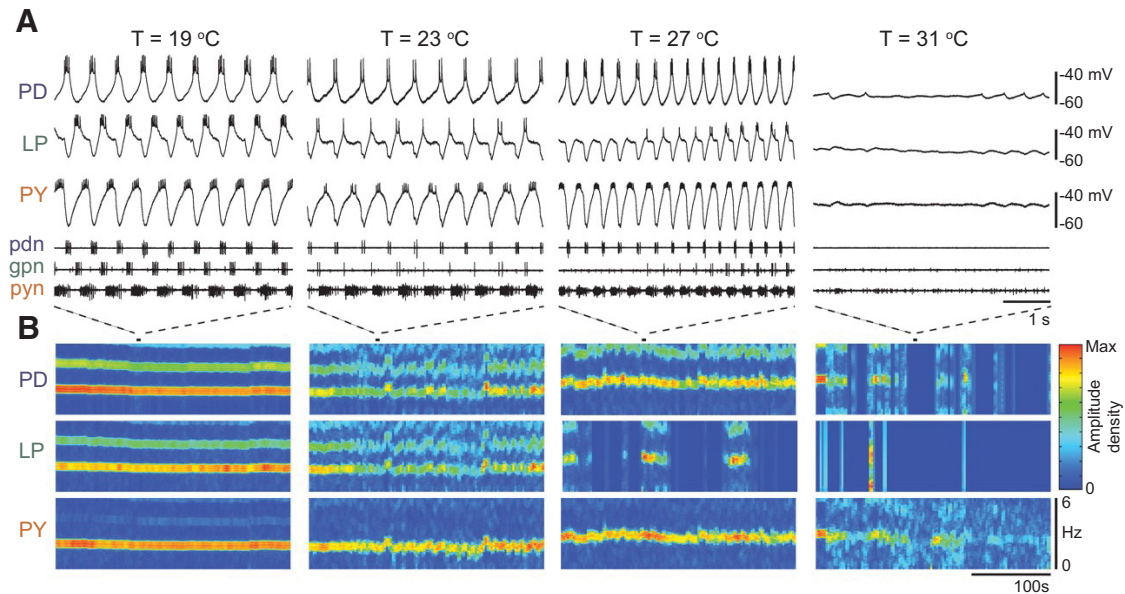


Figure 4. The pyloric rhythm is normal at 19°C but becomes disordered and crashes at higher temperatures. **A**, Simultaneous intracellular and extracellular recordings showing the triphasic rhythm at different recording temperatures. **B**, Power spectra showing frequency of the rhythm over 200 s of recordings. Data from Tang et al. (2012).

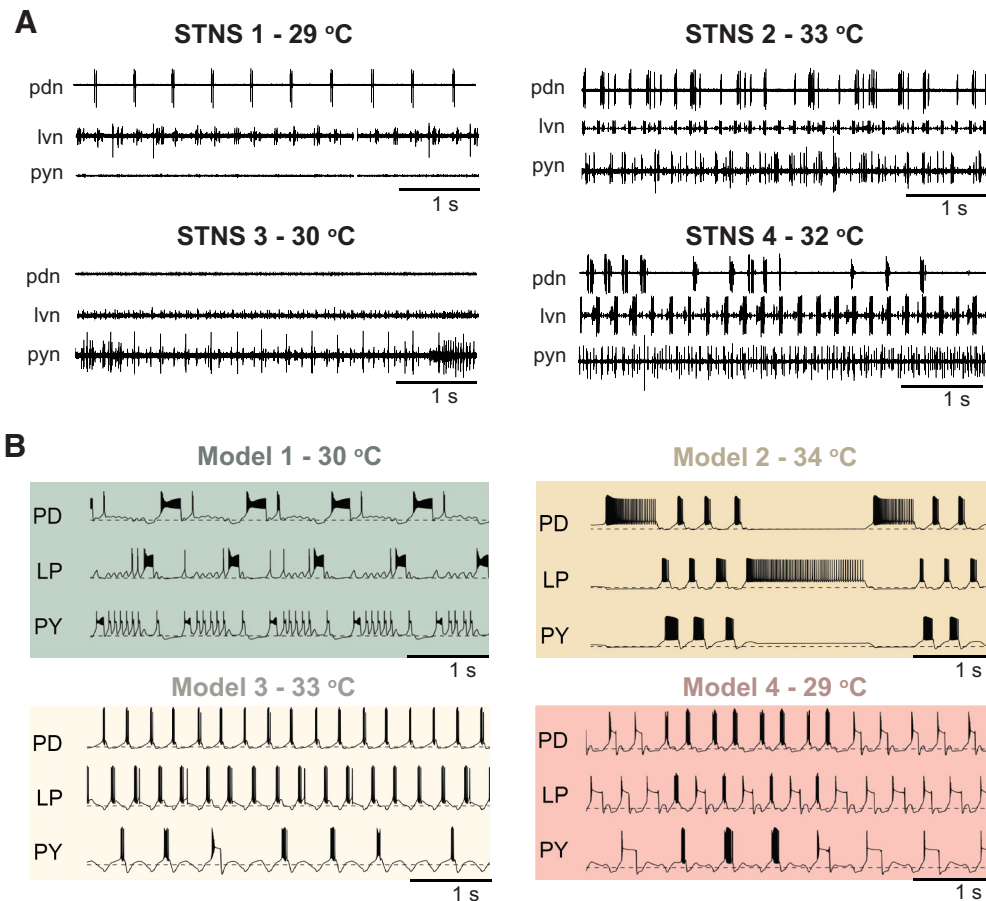


Figure 5. Individual pyloric rhythms exhibit different sensitivity to extreme temperatures and have distinct activity patterns on crash. **A**, PD, LP, and PY neuron activity in four STNS obtained from simultaneous extracellular recordings (pdn, lvn, and pyn, respectively). For all animals, the STNS exhibited normal triphasic pyloric activity at temperatures lower than the recording shown. Unpublished data from M.R. **B**, PD, LP, and PY neuron activity in four computational models of the pyloric circuit at high temperatures. All models also exhibited normal triphasic activity over the range of temperatures lower than the traces shown. Modified from Alonso and Marder (2020).

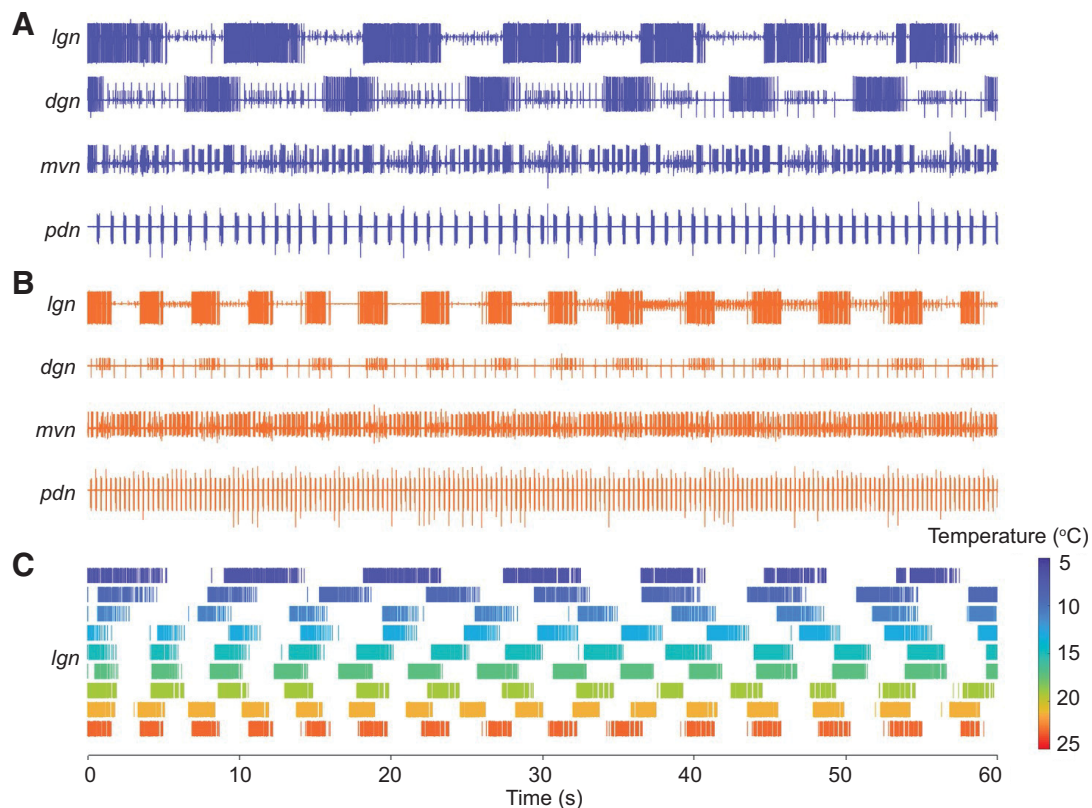


Figure 6. Temperature dependence of the gastric mill rhythm. **A, B**, Extracellular recordings of gastric mill rhythms from the same STNS at 7°C (blue) and 23°C (orange). **C**, Spike rasters showing the activity of the LG neuron over the entire temperature range. The first row in **C** corresponds to **A**, and the last row corresponds to **B**. Data from Powell et al. (2021).

The robustness of both rhythms is enhanced by neuromodulation (Städle et al., 2015; Haddad and Marder, 2018; DeMaegd and Stein, 2021), and it is possible that neuromodulation compensates for the extensive variability revealed when modulatory inputs are removed (Hamood and Marder, 2014, 2015; Haddad and Marder, 2018; Hamood et al., 2015).

Do global perturbations such as temperature reveal cryptic animal–animal differences?

Marine animals that deal with fluctuations in water temperature have many acclimation mechanisms that allow them to adapt to changes in environmental temperatures. Conventional wisdom argues that most acclimation takes place over 3–4 weeks. On the basis of this literature, Tang et al. (2012) acclimated animals in the laboratory for 3–5 weeks, and saw no appreciable changes in the pyloric rhythm at temperatures between 7°C and 23°C, but that animals acclimated to 19°C were more robust to high temperatures than animals acclimated at 7°C or 11°C.

Our early work on the effects of temperature was done from 2006 to 2010. The green recordings in Figure 7A show data from 2006 taken by Tang et al. (2010, 2012). This preparation showed normal activity at 11°C and 21°C but crashed at 31°C. One of the first indications that the pyloric rhythm crash temperatures may be similar to the proverbial “canary in the mine” with regard to ocean warming came with recordings that Haddad made in 2012 (Fig. 7A, blue). These recordings followed a winter during which the average water temperature was substantially warmer than usual (Marder et al., 2015). Note the normal rhythms at 31°C and 35°C. In Ratliff’s 2016 recordings (black), the crash temperature had returned to levels closer to those seen in 2006.

Disconcertingly, in 2021 (purple recordings), Rue and Li (unpublished data) recorded normal pyloric rhythms at temperatures as high as 39°C–40°C.

Despite the shifts in the crash temperature, at lower temperatures, there is relatively little difference between the frequencies of the pyloric rhythms (Fig. 7B), as originally reported by Tang et al. (2012) for laboratory-acclimated animals. Figure 7C plots the frequencies at crash for animals from the 2016–2017 year and for 2020–2021, and shows a significant upward shift in the frequency just before crash for 2020–2021. Likewise, the crash temperature is shifted up in the later dataset (Fig. 7D). The frequency at crash is plotted against crash temperature (Fig. 7E), and shows that there appears to be an almost linear relationship between crash temperature and crash frequency. It is perhaps not surprising that the long-term acclimation seen over many months in the ocean appears to be more extensive and long-lasting than that achieved with 4 weeks in the laboratory under controlled conditions.

The National Oceanic and Atmospheric Administration (NOAA) monitors ocean temperature continuously with sea buoys, and publishes these data on their website (https://www.ndbc.noaa.gov/station_history.php?station=44013). We pulled NOAA data for a buoy 16 nautical miles from Boston and likely within the catch area of the *C. borealis* studied here. Figure 7F, G shows the average summer and winter water temperatures from 1985 to 2021, with colored dots corresponding to the years of the recordings shown in Figure 7A. There is a systematic relationship between ocean temperature and the crash temperatures we measured from *in vivo* preparations made during those times.

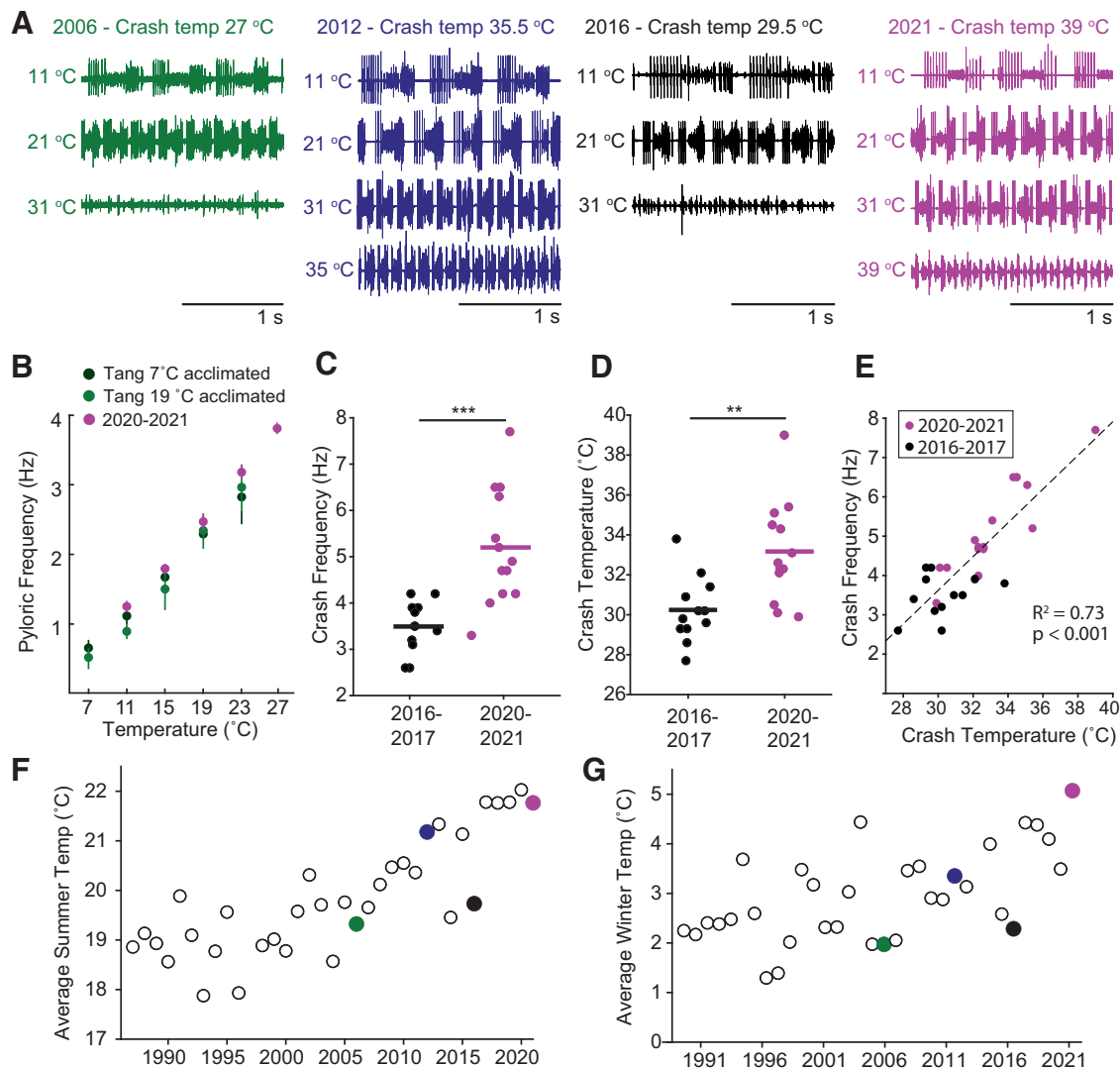


Figure 7. *A*, Extracellular recordings from temperature ramps to crash from four experiments performed over the last 15 years. Data come from reanalysis of recordings made by Sara Haddad, Lamont Tang, Jacob Ratliff, Janis Li, and M.R. All traces represent extracellular recordings from the lvn nerve at 11°C (control), 21°C, and 31°C. For preparations that were robust at 31°C, we also show the last temperature step at which the preparation was still robustly triphasic. *B*, Adapted from Tang et al. (2012). The pyloric network frequency plotted as a function of acute temperature for warm-acclimated (19°C; $N = 12$) and cold-acclimated (7°C; $N = 11$) animals recorded from between 2006 and 2010 compared with nonacclimated animals recorded from in 2020–2021 ($N = 13$). Error bars indicate SEM. *C*, *D*, Analysis from STNS exposed to temperature ramps up to crash performed in either 2016–2017 ($N = 12$) or 2020–2021 ($N = 13$). *C*, Maximum pyloric frequency before crash was significantly higher in 2020–2021 compared with 2016–2017 ($t_{(24)} = 4.38$, $p = 2.16 \times 10^{-4}$). *D*, Maximum temperature at crash was significantly higher in 2020–2021 compared with 2016–2017 ($t_{(24)} = 3.41$, $p = 0.0024$). *E*, Maximum frequency before crash plotted against the temperature at crash. *F*, *G*, Average summer (June – August) and winter (December – February) sea temperatures 16NM East of Boston from 1985–2021. Winter temperature years correspond to the February date. Colored dots represent the seasons from which we show example traces and analysis above (A–E). Data were compiled from NOAA (https://www.ndbc.noaa.gov/station_history.php?station=44013). $**p < 0.01$, $***p < 0.001$.

An unanswered question: are some sets of parameters associated with higher resilience?

We do not yet know whether there are specific patterns of mRNA expression levels in individuals that are more robust to temperature, or to other perturbations. We hope in the future to use improved molecular analyses and theory studies to answer this question.

Conclusion

It is disconcerting that we might never have been aware of the long-term changes in the nervous systems of the crabs we study had we only studied them under constant, well-defined, standard conditions. Of course, these standardized conditions were designed to remove fluctuations because of random changes in how the experiments were done, and ensured baseline data from thousands of animals, thus allowing us and others to compare

experiments done many years apart. Nonetheless, there are always anecdotal conversations among community members mumbling about changes in this or that response to a modulator or stimulation.

It is clear that robust baseline data can hide a number of experience-dependent changes that can influence an animal's behavior. That said, a recent analysis of large amounts of data from multiple investigators and multiple laboratories (Gorur-Shandilya et al., 2021) showed that control data were independent of investigator and laboratory origin. Thus, the yearly trends in differential resilience to temperature extremes reported here are likely to reflect the state of the wild-caught animals and their temperature history. After the winter of 2012, there were reports of animal species who migrated north to Maine from Massachusetts in search of colder waters. But not all species can, or do, relocate over large distances to seek their preferred

environments. Instead, it is likely that the population is enriching for those animals that are more warm water resilient by either adaptation, attrition, or a combination of both. But a concern is that this increased tolerance for warmer ocean temperatures may come at a cost of robustness to other perturbations, and this potential decrease in resilience to other perturbations may also be invisible or “cryptic” under control conditions.

References

- Alonso LM, Marder E (2019) Visualization of currents in neural models with similar behavior and different conductance densities. *eLife* 8:e42722.
- Alonso LM, Marder E (2020) Temperature compensation in a small rhythmic circuit. *eLife* 9:e55470.
- Amendola J, Woodhouse A, Martin-Eauclaire MF, Goaillard JM (2012) Ca^{2+} /cAMP-sensitive covariation of I_A and I_H voltage dependences tunes rebound firing in dopaminergic neurons. *J Neurosci* 32:2166–2181.
- Beenhakker MP, Blitz DM, Nusbaum MP (2004) Long-lasting activation of rhythmic neuronal activity by a novel mechanosensory system in the crustacean stomatogastric nervous system. *J Neurophysiol* 91:78–91.
- Beenhakker MP, Kirby MS, Nusbaum MP (2007) Mechanosensory gating of proprioceptor input to modulatory projection neurons. *J Neurosci* 27:14308–14316.
- Blitz DM, Nusbaum MP (2012) Modulation of circuit feedback specifies motor circuit output. *J Neurosci* 32:9182–9193.
- Buchholtz F, Golowasch J, Epstein IR, Marder E (1992) Mathematical model of an identified stomatogastric ganglion neuron. *J Neurophysiol* 67:332–340.
- Caplan JS, Williams AH, Marder E (2014) Many parameter sets in a multi-compartment model oscillator are robust to temperature perturbations. *J Neurosci* 34:4963–4975.
- DeMaegd ML, Stein W (2021) Neuropeptide modulation increases dendritic electrical spread to restore neuronal activity disrupted by temperature. *J Neurosci* 41:7607–7622.
- Edelman GM, Gally JA (2001) Degeneracy and complexity in biological systems. *Proc Natl Acad Sci USA* 98:13763–13768.
- Epstein IR, Marder E (1990) Multiple modes of a conditional neural oscillator. *Biol Cybern* 63:25–34.
- Goaillard JM, Marder E (2021) Ion channel degeneracy, variability, and covariation in neuron and circuit resilience. *Annu Rev Neurosci* 44:335–357.
- Goaillard JM, Taylor AL, Schulz DJ, Marder E (2009) Functional consequences of animal-to-animal variation in circuit parameters. *Nat Neurosci* 12:1424–1430.
- Goldman MS, Golowasch J, Marder E, Abbott LF (2001) Global structure, robustness, and modulation of neuronal models. *J Neurosci* 21:5229–5238.
- Golowasch J (2014) Ionic current variability and functional stability in the nervous system. *Bioscience* 64:570–580.
- Golowasch J, Marder E (1992) Ionic currents of the lateral pyloric neuron of the stomatogastric ganglion of the crab. *J Neurophysiol* 67:318–331.
- Golowasch J, Buchholtz F, Epstein IR, Marder E (1992) Contribution of individual ionic currents to activity of a model stomatogastric ganglion neuron. *J Neurophysiol* 67:341–349.
- Golowasch J, Goldman MS, Abbott LF, Marder E (2002) Failure of averaging in the construction of a conductance-based neuron model. *J Neurophysiol* 87:1129–1131.
- Gorur-Shandilya S, Cronin EM, Schneider AC, Haddad SA, Rosenbaum P, Bucher D, Nadim F, Marder E (2021) Mapping circuit dynamics during function and dysfunction. *bioRxiv* 451370. doi: 10.1101/2021.07.06.451370.
- Guckenheimer J, Gueron S, Harris-Warrick RM (1993) Mapping the dynamics of a bursting neuron. *Philos Trans R Soc Lond B Biol Sci* 341:345–359.
- Guckenheimer J, Harris-Warrick R, Peck J, Willms A (1997) Bifurcation, bursting, and spike frequency adaptation. *J Comput Neurosci* 4:257–277.
- Haddad SA, Marder E (2018) Circuit robustness to temperature perturbation is altered by neuromodulators. *Neuron* 100:609–623.
- Haley JA, Hampton D, Marder E (2018) Two central pattern generators from the crab, *Cancer borealis*, respond robustly and differentially to extreme extracellular pH. *eLife* 7:e41877.
- Hamood AW, Haddad SA, Otopalik AG, Rosenbaum P, Marder E (2015) Quantitative reevaluation of the effects of short- and long-term removal of descending modulatory inputs on the pyloric rhythm of the crab, *Cancer borealis*. *eNeuro* 2:ENEURO.0058-14.2015.
- Hamood AW, Marder E (2014) Animal-to-animal variability in neuromodulation and circuit function. *Cold Spring Harb Symp Quant Biol* 79:21–28.
- Hamood AW, Marder E (2015) Consequences of acute and long-term removal of neuromodulatory input on the episodic gastric rhythm of the crab *Cancer borealis*. *J Neurophysiol* 114:1677–1692.
- He LS, Rue MC, Morozova EO, Powell DJ, James EJ, Kar M, Marder E (2020) Rapid adaptation to elevated extracellular potassium in the pyloric circuit of the crab, *Cancer borealis*. *J Neurophysiol* 123:2075–2089.
- LeMasson G, Marder E, Abbott LF (1993) Activity-dependent regulation of conductances in model neurons. *Science* 259:1915–1917.
- Liu Z, Golowasch J, Marder E, Abbott LF (1998) A model neuron with activity-dependent conductances regulated by multiple calcium sensors. *J Neurosci* 18:2309–2320.
- Marder E, Bucher D (2007) Understanding circuit dynamics using the stomatogastric nervous system of lobsters and crabs. *Annu Rev Physiol* 69:291–316.
- Marder E, Taylor AL (2011) Multiple models to capture the variability in biological neurons and networks. *Nat Neurosci* 14:133–138.
- Marder E, Haddad SA, Goeritz ML, Rosenbaum P, Kispersky T (2015) How can motor systems retain performance over a wide temperature range? Lessons from the crustacean stomatogastric nervous system. *J Comp Physiol A Neuroethol Sens Neural Behav Physiol* 201:851–856.
- Moubarak E, Engel D, Dufour MA, Tapia M, Tell F, Goaillard JM (2019) Robustness to axon initial segment variation is explained by somatodendritic excitability in rat substantia nigra dopaminergic neurons. *J Neurosci* 39:5044–5063.
- Northcutt AJ, Kick DR, Otopalik AG, Goetz BM, Harris RM, Santin JM, Hofmann HA, Marder E, Schulz DJ (2019) Molecular profiling of single neurons of known identity in two ganglia from the crab *Cancer borealis*. *Proc Natl Acad Sci USA* 116:26980–26990.
- O’Leary T, Marder E (2016) Temperature-robust neural function from activity-dependent ion channel regulation. *Curr Biol* 26:2935–2941.
- O’Leary T, Williams AH, Caplan JS, Marder E (2013) Correlations in ion channel expression emerge from homeostatic tuning rules. *Proc Natl Acad Sci USA* 110:E2645–E2654.
- O’Leary T, Williams AH, Franci A, Marder E (2014) Cell types, network homeostasis, and pathological compensation from a biologically plausible ion channel expression model. *Neuron* 82:809–821.
- Otopalik AG, Sutton AC, Banghart M, Marder E (2017a) When complex neuronal structures may not matter. *eLife* 6:e23508.
- Otopalik AG, Goeritz ML, Sutton AC, Brookings T, Guerini C, Marder E (2017b) Sloppy morphological tuning in identified neurons of the crustacean stomatogastric ganglion. *eLife* 6:e22352.
- Otopalik AG, Pipkin J, Marder E (2019) Neuronal morphologies built for reliable physiology in a rhythmic motor circuit. *eLife* 8:e41728.
- Powell DJ, Haddad SA, Gorur-Shandilya S, Marder E (2021) Coupling between fast and slow oscillator circuits in *Cancer borealis* is temperature-compensated. *eLife* 10:e60454.
- Prinz AA, Billimoria CP, Marder E (2003) Alternative to hand-tuning conductance-based models: construction and analysis of databases of model neurons. *J Neurophysiol* 90:3998–4015.
- Prinz AA, Bucher D, Marder E (2004) Similar network activity from disparate circuit parameters. *Nat Neurosci* 7:1345–1352.
- Ratcliff J, Franci A, Marder E, O’Leary T (2021) Neuronal oscillator robustness to multiple global perturbations. *Biophys J* 120:1454–1468.
- Rinberg A, Taylor AL, Marder E (2013) The effects of temperature on the stability of a neuronal oscillator. *PLoS Comput Biol* 9:e1002857.
- Robertson RM, Money TG (2012) Temperature and neuronal circuit function: compensation, tuning and tolerance. *Curr Opin Neurobiol* 22:724–734.
- Roffman RC, Norris BJ, Calabrese RL (2012) Animal-to-animal variability of connection strength in the leech heartbeat central pattern generator. *J Neurophysiol* 107:1681–1693.
- Schulz DJ, Goaillard JM, Marder E (2006) Variable channel expression in identified single and electrically coupled neurons in different animals. *Nat Neurosci* 9:356–362.
- Schulz DJ, Goaillard JM, Marder EE (2007) Quantitative expression profiling of identified neurons reveals cell-specific constraints on

- highly variable levels of gene expression. *Proc Natl Acad Sci USA* 104:13187–13191.
- Soofi W, Goeritz ML, Kispersky TJ, Prinz AA, Marder E, Stein W (2014) Phase maintenance in a rhythmic motor pattern during temperature changes in vivo. *J Neurophysiol* 111:2603–2613.
- Städle C, Heigle S, Stein W (2015) Neuromodulation to the rescue: compensation of temperature-induced breakdown of rhythmic motor patterns via extrinsic neuromodulatory input. *PLoS Biol* 13:e1002265.
- Tang LS, Goeritz ML, Caplan JS, Taylor AL, Fisek M, Marder E (2010) Precise temperature compensation of phase in a rhythmic motor pattern. *PLoS Biol* 8:e1000469.
- Tang LS, Taylor AL, Rinberg A, Marder E (2012) Robustness of a rhythmic circuit to short- and long-term temperature changes. *J Neurosci* 32:10075–10085.
- Tapia M, Baudot P, Formisano-Treziny C, Dufour MA, Temporal S, Lasserre M, Marqueze-Pouey B, Gabert J, Kobayashi K, Goaillard JM (2018) Neurotransmitter identity and electrophysiological phenotype are genetically coupled in midbrain dopaminergic neurons. *Sci Rep* 8:13637.
- Taylor AL, Hickey TJ, Prinz AA, Marder E (2006) Structure and visualization of high-dimensional conductance spaces. *J Neurophysiol* 96:891–905.
- Taylor AL, Goaillard JM, Marder E (2009) How multiple conductances determine electrophysiological properties in a multicompartment model. *J Neurosci* 29:5573–5586.
- Temporal S, Desai M, Khorkova O, Varghese G, Dai A, Schulz DJ, Golowasch J (2012) Neuromodulation independently determines correlated channel expression and conductance levels in motor neurons of the stomatogastric ganglion. *J Neurophysiol* 107:718–727.
- Turrigiano GG, LeMasson G, Marder E (1995) Selective regulation of current densities underlies spontaneous changes in the activity of cultured neurons. *J Neurosci* 15:3640–3652.